Electronic Supplementary Material (ESI) for Journal of Materials Chemistry B.

Supporting Information for

Highly Photoluminescent Superparamagnetic Silica Composites for on-Site Biosensor

Wooyoung Park, Mi Jung Kim, Yuri Choe, Sang Kyung Kim*, and Kyoungja Woo*

Abbreviations

M	magnetic core
MS	magnetic core surrounded with thick silica shell
Q	self-assembled quantum dot (QD) layer
MSQ	**MS** with **Q**
MSQS	**MSQ** coated with a thin silica shell
A	aptamer
qDNA	quencher-bonded oligo-DNA
qA	quencher-bonded **A**
T	thrombin
MSQS-A	**MSQS** with immobilized **A**s
MSQS-A/qDNA	**MSQS-A** hybridized with **q**DNAs through **A**
MSQS-A/T	**MSQS-A** bonded to **T** through **A**

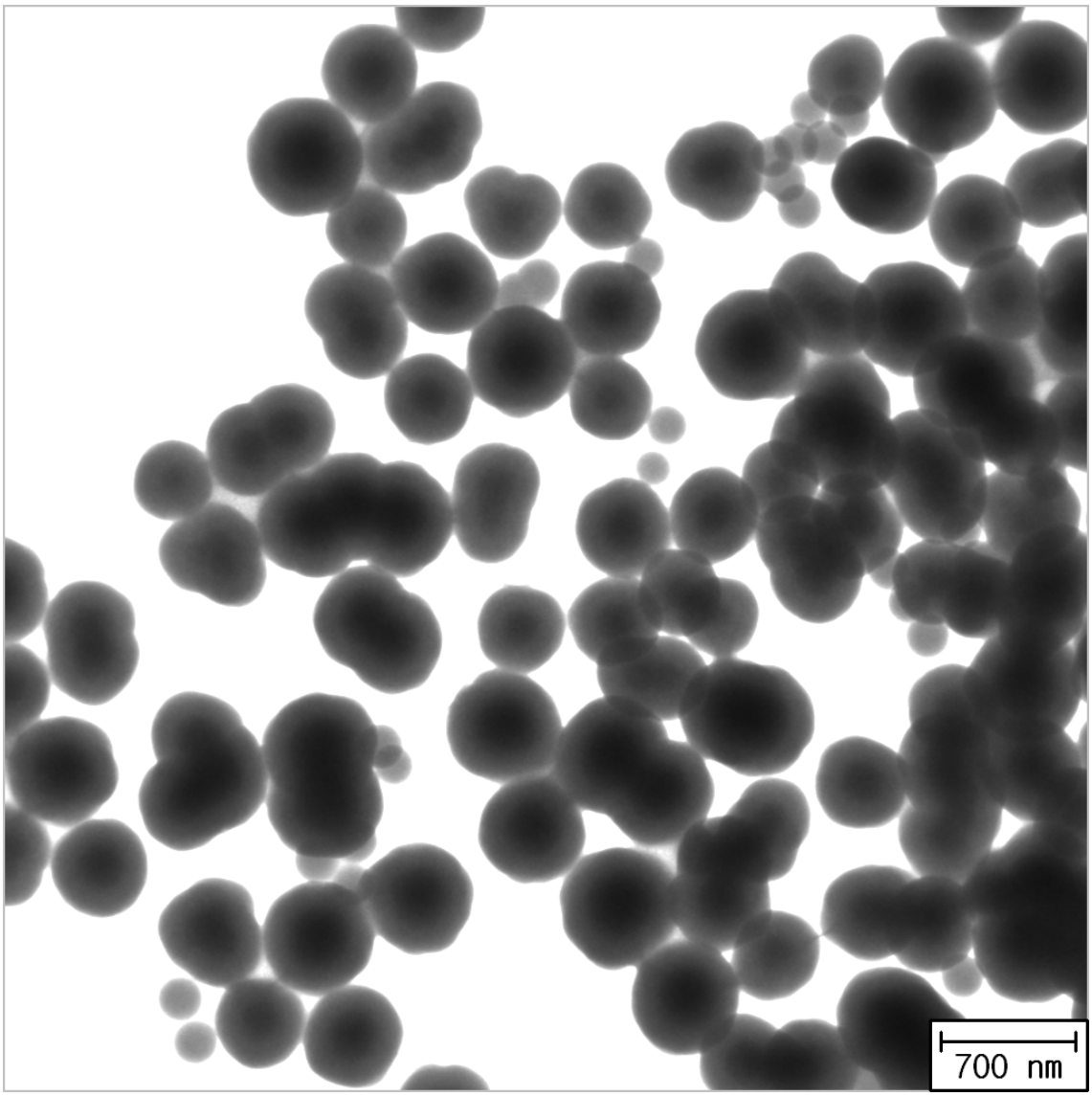

Figure S1. TEM image of many AP − **MS** particles.

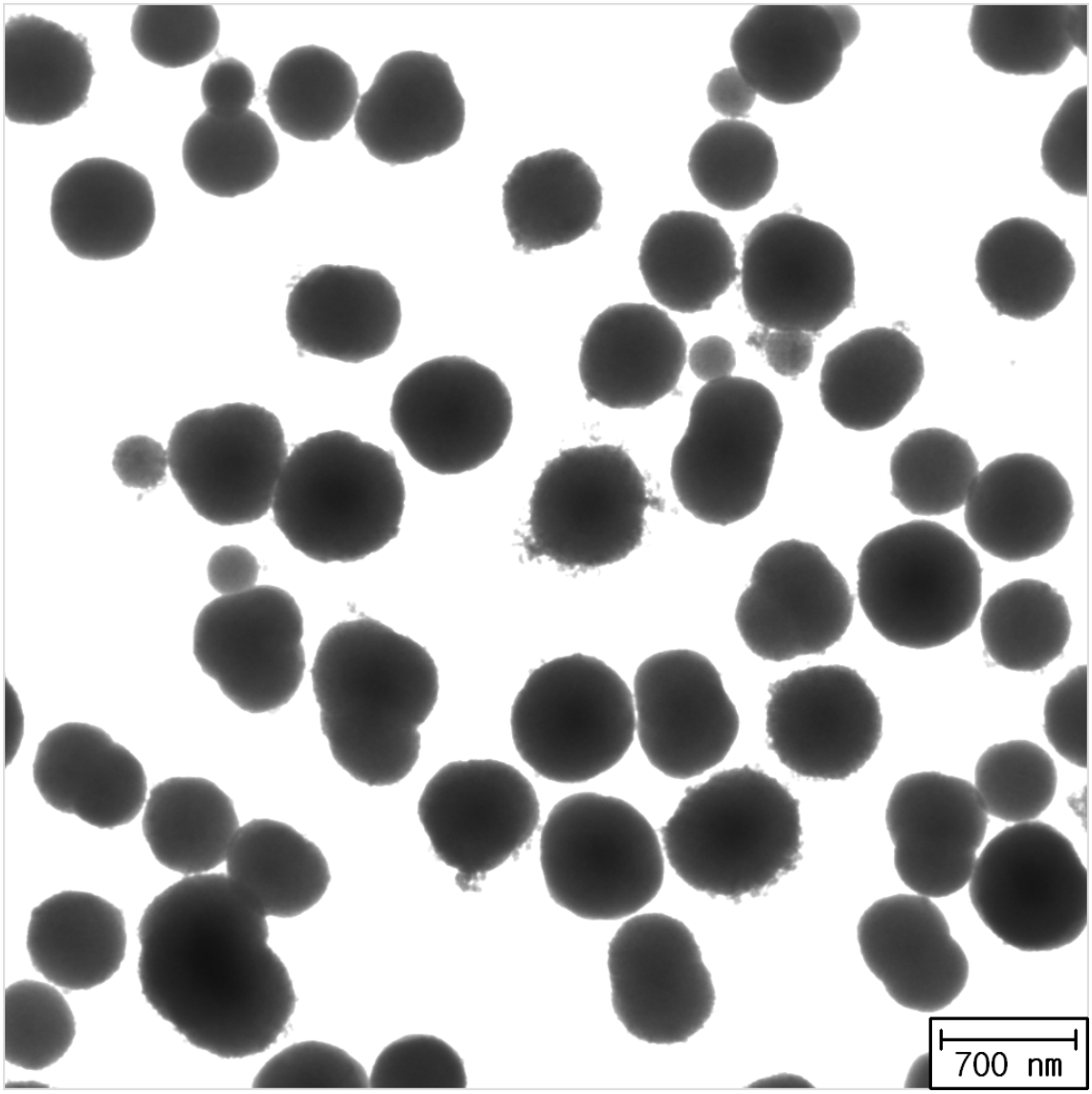

Figure S2. TEM image of many **MSQS** particles. (Average diameter ± STD = 568 ± 78 nm)

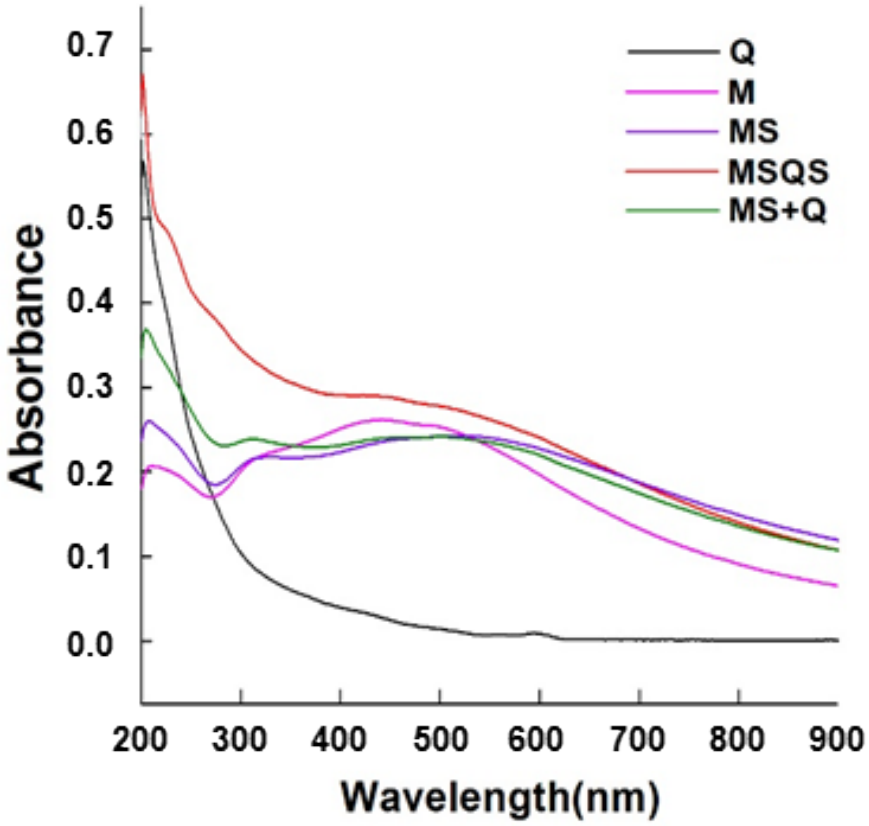

Figure S3. Absorption spectra of **Q** and **MSQS** analogues in the visible range.

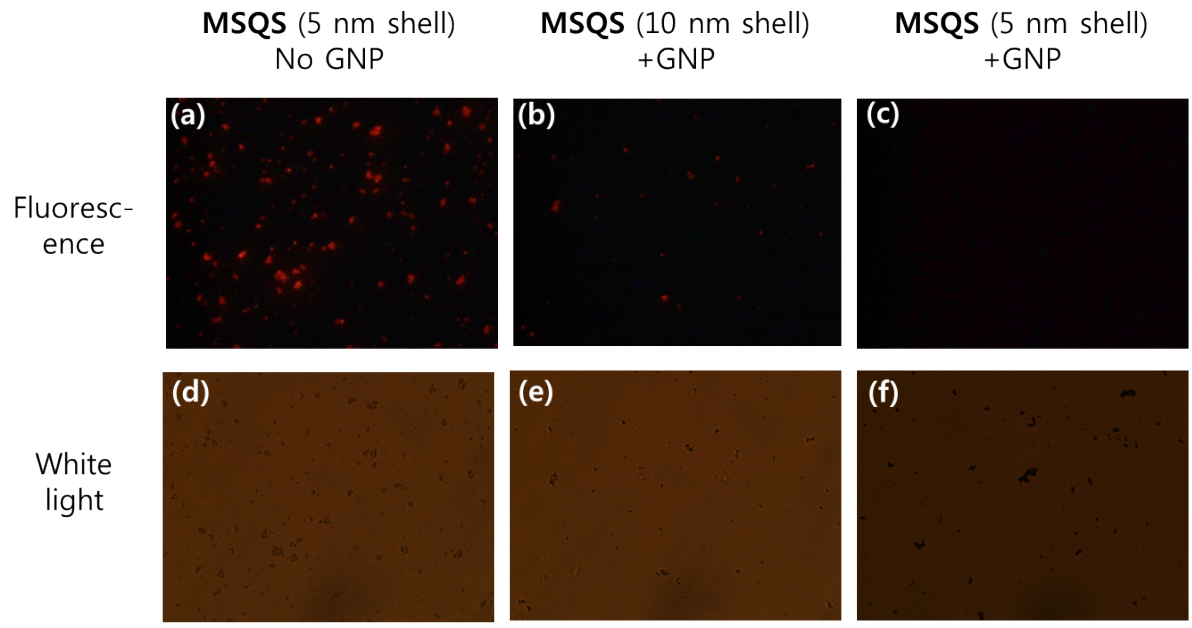

*GNP : Gold Nano-Particle, diameter=15 nm

Figure S4. Quenching the fluorescence of AP-**MSQS** with GNP to evaluate the effect of silica shell thickness. AP-**MSQS** of 5 nm shell was quenched completely with GNP while the AP-**MSQS** of 10 nm shell emitted dim fluorescence. (0.1 μg **MSQS** + 10 fmole GNP)

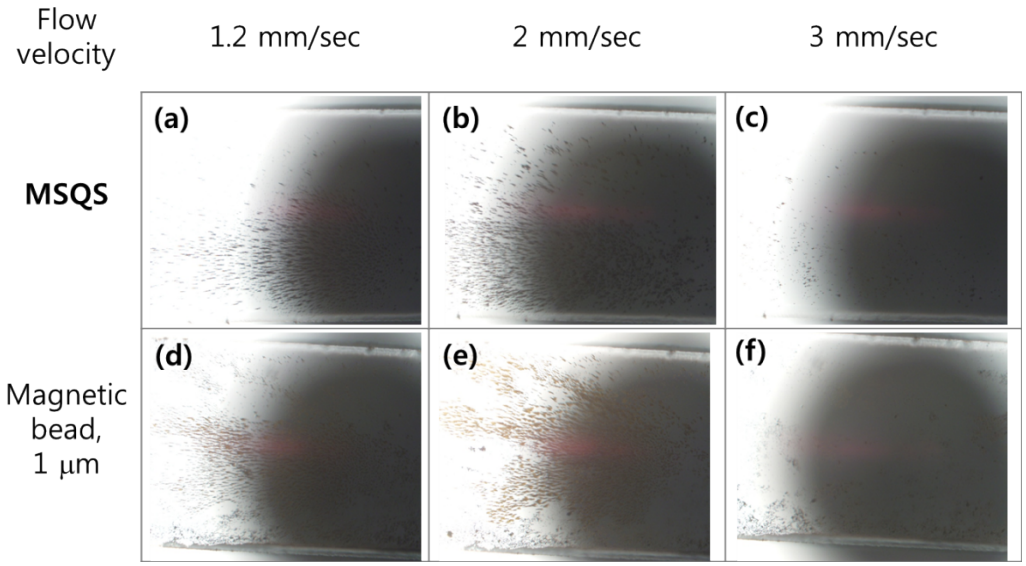

Figure S5. **MSQS** and commercial magnetic particles (Dynabeads MyOne®, Invitrogen) in a magnetophoretic channel. Magnetic susceptibility of the commercial magnetic particle provided by the vendor was 0.064 emu·g^{-1} , which is much less than that of **MSQS**, 7 emu·g^{-1}. The width and height of the channel were 500 μm and 80 μm, respectively. NdFeB magnet of 1 mm diameter was placed 1 mm apart from the bottom of the channel. Both of the magnetic particles could not withstand water flow over 3 mm·sec^{-1}, implying similar magnetic capturing efficiencies.

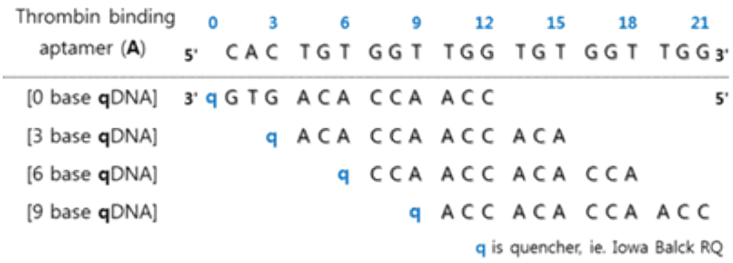

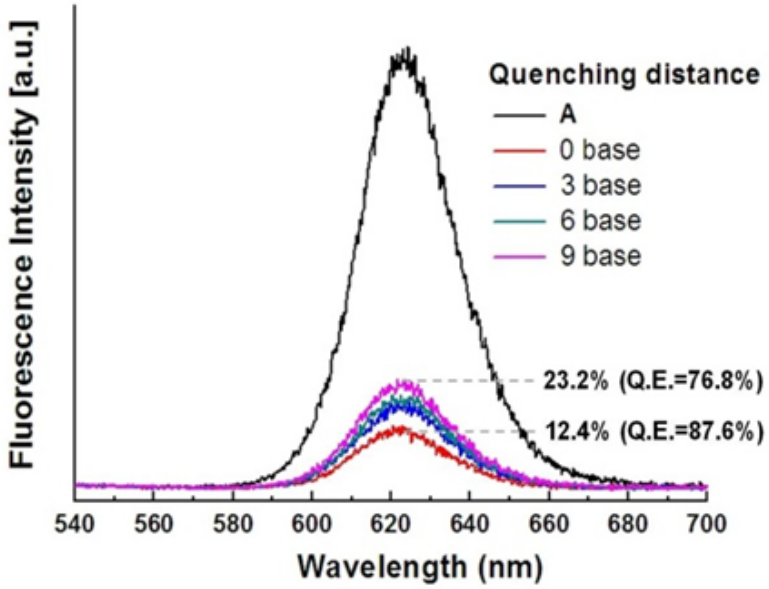

Figure S6. Fluorescence spectra from QDs modified with the aptamer and quenchers. Position of quencher varies from base 0 to base 9.

The thrombin binding aptamer was immobilized covalently on the QD, and the position of the quencher varied by three bases . The hybridization of **q**DNA was then varied by three bases. For single-stranded DNAs, each base is estimated to be 5 Å long. Thus, the nine-base quencher is about 5 nm from the QD surface. The hybridization of **q**DNA was carried out by incubation for 2 min at 50 ºC and then, natural cooling for 30 min to 25 ºC.

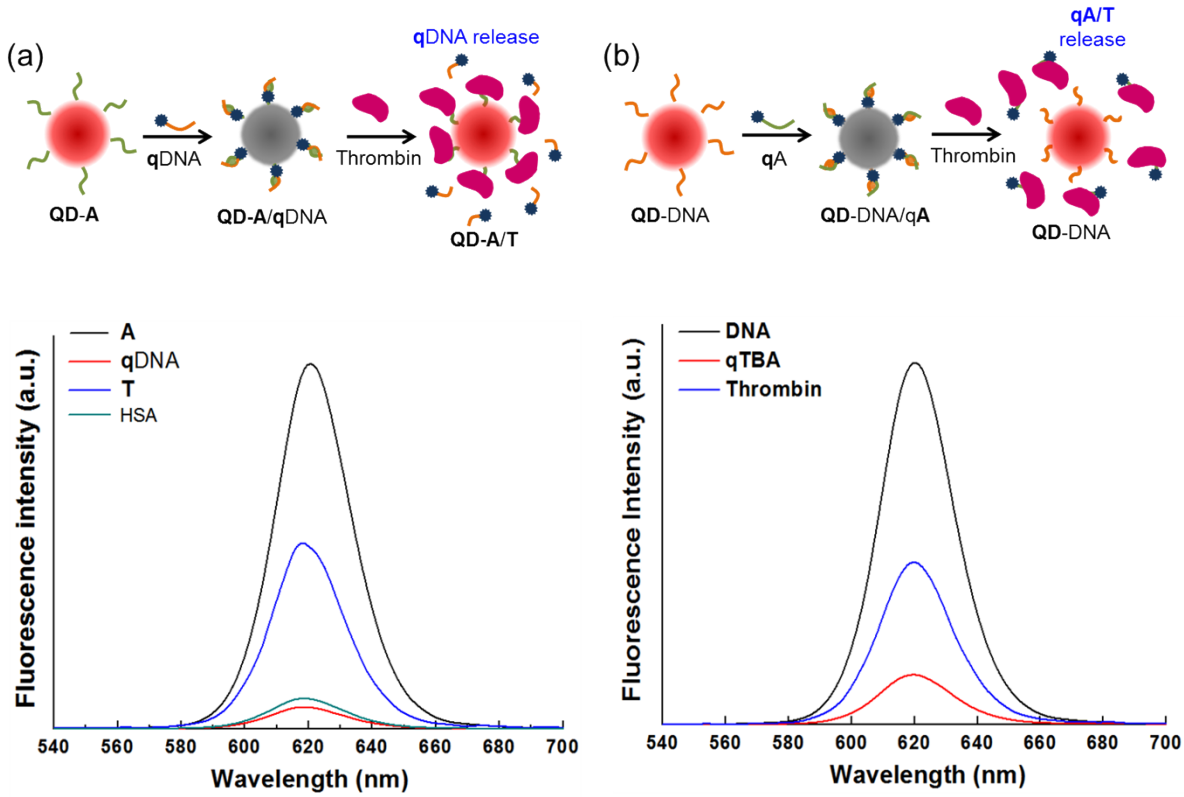

Figure S7. PL from QD solution at each step of immobilization, hybridization, and single-step assay (protein 90 μg·mL^{-1}). Two configurations are compared; (a) **A**-immobilized QD and (b) DNA-immobilized QD.

The configuration of aptamers (**A**s) and quenchers (**q**s) was investigated on QDs for better target binding and fluorescent signaling. Thrombin binding aptamer (**A**) was immobilized on QDs and **q**DNA was hybridized to **A** as in figure S7 (a). Another set of QDs was prepared where the position of **A** and DNA switched as in Figure S7 (b). The quencher-free DNA was immobilized on QDs and quencher-TBA (**qA**) was hybridized to DNA. Now, to recover the fluorescence of QDs, either **q**DNAs or **qA**/**T** complexes were released as described in Figure S7 (a) and (b). As expected, the **qA** could be hybridized to DNA and extinct fluorescence from QDs. However, the resultant quenching efficiency decreased by 8% (94% in (a) and 86% in (b)). The relatively bulky and negatively charged TBA seems to be less favorable to be concentrated on the surface

of a particle with the same hybridization energy of 12 bases (~20 kcal·mol^{-1}). Owing to the configurational differences, the ratio of fluorescent signal to background noise level could be varied from 3.2 (b) to 8.5 (a). The fluorescence intensity was measured after 5 minute-incubation of 200 μL of binding buffer where the concentration of proteins and QD were 100 μg·mL^{-1} and 225 nM, respectively.